Incisor enamel microstructure of hystricognathous and anomaluroid rodents from the earliest Oligocene of Dakhla, Atlantic Sahara (Morocco)

Laurent Marivaux, Myriam Boivin, Sylvain Adnet, Mohamed Benammi, Rodolphe Tabuce, Mouloud Benammi

Incisor enamel microstructure of hystricognathous and anomaluroid rodents from the earliest Oligocene of Dakhla, Atlantic Sahara (Morocco)

Laurent Marivaux[1], Myriam Boivin[1], Sylvain Adnet[1], Mohamed Benammi[2], Rodolphe Tabuce[1] & Mouloud Benammi[3]

[1] Laboratoire de Paléontologie, Institut des Sciences de l'Évolution de Montpellier (ISE-M, UMR 5554, CNRS/UM/IRD/EPHE), c.c. 064, Université de Montpellier, place Eugène Bataillon, F-34095 Montpellier Cedex 05, France

[2] Laboratoire de Géologie Géophysique Géorisques et Environnement (3GE), Université Ibn Tofail, Faculté des Sciences, BP. 133, Kénitra 14000, Morocco

[3] Institut de Paléoprimatologie, Paléontologie Humaine : Évolution et Paléoenvironnements (iPHEP, UMR-CNRS 7262), Université de Poitiers UFR SFA, 40 avenue du Recteur Pineau, F-86022 Poitiers Cedex, France

Corresponding author: Laurent Marivaux

Laurent.Marivaux@UMontpellier.fr

ORCID numbers:

- Laurent Marivaux: 0000-0002-2882-0874
- Myriam Boivin: 0000-0002-5240-9460

Abstract

Seven hystricognaths and five anomaluroids have been recently described from the earliest Oligocene of the Dakhla (DAK C_2) region of Morocco, based primarily on isolated cheek teeth. Here, we analyzed the enamel microstructure of thirty associated isolated fragments of incisors. Among these specimens, only three display an early stage of uniserial Hunter-Schreger bands (HSBs), with mostly a single prism per band, but also occasionally two prisms per band (in two specimens), and a thin interprismatic matrix (IPM) that runs parallel to the prism direction, thereby documenting incisors of anomaluroids. All other sampled incisors display an enamel with multiserial HSBs, thereby documenting hystricognaths. For these latter, we recorded primarily an IPM crystallite arrangement describing the subtype 2 of multiserial HSBs, but with variation including a wide amplitude in the angle (acute) formed between the crystallites of IPM and those of the prisms, some variations in the frequency of the IPM sheet anastomoses, in the number of prisms per HSBs, and variations in the inclination of the HSBs. The absence of the subtypes 2-3 and 3 of multiserial HSBs in DAK C_2 suggests that African hystricognathous rodents had still not achieved these most resistant multiserial HSBs at that time. The drier, cooler climatic regime of the early Oligocene, having increased the fragmentation and opening of habitats, might have played a role in the subsequent selection of taxa having acquired a more resistant incisor enamel.

Keywords

Africa; Paleogene; Rodentia; uniserial; multiserial

Introduction

In the framework of our paleontological research program in North Africa, since 2009 we have concentrated some of our field efforts in the westernmost part of the Sahara, notably on the geological outcrops of the upper Samlat Formation, exposed on the mainland shoreline of the Rio de Oro, east of the Dakhla peninsula, Morocco (Fig. 1). Our paleontological surveys have allowed for the discovery of the first Paleogene record of rodents from the Atlantic margin of North Africa (Marivaux et al. 2017a,b). The fossils come from a single stratigraphic level (Dakhla C_2 [DAK C_2]; Adnet et al. 2017; Benammi et al. 2017; Marivaux et al. 2017a,b), which is particularly well exposed and accessible in two sections (Porto Rico [Pto] and El Argoub [Arg]; Fig. 1), situated in a limited area, about 20 km east of the Dakhla city. In both sections, this fossil-bearing level corresponds to estuarine deposits, which were dated to the earliest Oligocene by chemostratigraphy (Benammi et al. 2017; Noiret et al. 2017). Wet-screening of several tons of sediment (Pto C_2: ca. 1,700 kg; Arg C_2: ca. 1,500 kg) have yielded in the two localities similar fossil assemblages of marine and estuarine invertebrates and vertebrates, together with terrestrial mammals including rodents, primates, and afrotherians. Rodents are documented by isolated teeth and few jaw and bone fragments, which illustrate members of two phylogenetically distinct groups: Anomaluroidea and Hystricognathi (the only rodent clades to be known/present in Africa at that time). More than a dozen isolated cheek teeth document five anomaluroid species (*Paranomalurus riodeoroensis*, *Argouburus minutus*, *Oromys zenkerellinopsis*, *Nonanomalurus parvus*, and *Dakhlamys ultimus*; see Marivaux et al. 2017a), and several tens of isolated cheek teeth plus three jaw fragments document at least seven species of hystricognaths (*Gaudeamus* cf. *G. aslius*, *Gaudeamus* cf. *G. hylaeus*, *Phenacophiomys occidentalis*, *Birkamys* aff. *B. korai*, *Mubhammys atlanticus*, *Neophiomys minutus*, and ?*Phiocricetomys* sp.; see Marivaux et al.

2017b). Whereas anomaluroid taxa provide an unprecedented taxonomic record of that rodent group in Africa at that time, hystricognaths primarily document close relatives of taxa that are known from Egyptian localities of the Jebel Qatrani Formation (Fayum Depression), either dating from the latest Eocene (L-41; Sallam et al. 2011; Sallam and Seiffert 2016) or from the early Oligocene (Wood 1968; see also Coster et al. 2012, for the report of earliest Oligocene hystricognaths from Libya, Zallah [Z5R locality]). This discovery provides a remarkable snapshot regarding the paleodiversity of anomaluroid and hystricognathous rodents at that time, which was so far only documented by fossil assemblages from northern and northeastern Africa (Libya, Egypt) and from Arabia (Dhofar in Oman). This new earliest Oligocene rodent fauna from the northern Atlantic margin of Africa (Atlantic Sahara) is therefore particularly critical for balancing the early Oligocene rodent fossil record of North Africa, and for a better understanding of the paleobiogeography of mammals at that time (Marivaux et al. 2017a,b). Furthermore, this unique assemblage demonstrates that rodents were particularly diversified near the global cooling recorded at the Eocene/Oligocene transition, thereby suggesting that this tropical region of North Africa was seemingly less affected by the climatic changes recorded at that time (e.g., Berggren and Prothero 1992; Coxall et al. 2005; Lear et al. 2008; Zachos et al. 2008; Hren et al. 2013; Tramoy et al. 2016).

In this paper, we continue the study of the DAK C_2 rodent fauna, in analyzing the enamel microstructure of several isolated incisors (lower and upper specimens). For Paleogene African (and Asian) hystricognaths and anomaluroids, this kind of analyses has so far been carried out only on a few specimens, primarily by Martin (1992, 1993, 1995; see also Martin in Coster et al., 2010), and on a more systematic basis by Marivaux et al. (2000, 2011, 2012, 2014, 2015, 2017a; see also Marivaux 2000 [unpublished PhD]), when rodent taxa were newly described or re-studied. Basically, the incisor enamel in rodents is primarily formed by two layers (Korvenkontio, 1934), the Portio interna (PI), which includes decussating prism

layers, named Hunter-Schreger bands (HSBs), and the Portio externa (PE), which consists of radial enamel (prisms are oriented in the same direction). From what is currently documented (extinct and extant species), all hystricognathous rodents (i.e., Old and New Worlds species [stem hystricognaths, phiomorphs, and caviomorphs]; ESM 1) display an incisor enamel characterized by a PI exhibiting decussating multi-prism layers (i.e., multiserial HSBs). In contrast, the incisor enamel of anomaluroids (ESM 2) is characterized by a PI having decussating one (to two, in primitive species) prism layers (i.e., uniserial HSBs). Initially, Martin (1992, 1993, 1994, 1997) distinguished three subtypes of multiserial HSBs, especially on the basis of the angle formed by the direction of the interprismatic crystallites (IPM) with respect to the prism long axes (see also Vieytes 2003; Vucetich and Vieytes 2006; Boivin et al. submitted). In the subtype 1, the IPM crystallites run parallel to those of the prisms, or form a very low angle with them, and anastomose very regularly (sheet to sheath-like IPM). In the subtype 2, the IPM crystallites form an acute angle and anastomose regularly, while in the subtype 3, the IPM shows a few or no anastomoses, and its crystallites run at a right angle to those of the prisms (plate-like IPM). The same is true for the uniserial HSBs, where different subtypes are observed in function of the angle of the IPM crystallites with respect to the prism long axes (e.g., Martin 1997). It has been argued that an increasing angulation of the IPM strengthens the enamel in the third dimensions, and that a rectangular IPM arrangement is the most derived and specialized condition as a result (better resistance to the crack propagations; Martin 1992, 1993, 1994, 1997). This biomechanical assumption is otherwise corroborated by the successive stratigraphic occurrences of the different subtypes (Martin 1994, 1997; see also Boivin et al. submitted and references herein).

Here, we selected, prepared, and analyzed some thirty isolated upper and lower rodent incisors of different sizes from DAK C_2 (Pto and Arg), in order to document a maximum of incisor enamel microstructural patterns recorded in this area at that time. With this large

sample analyzed, we expect to document as thoroughly as possible the evolutionary degrees characterizing the incisor enamel microstructural complexity in these earliest Oligocene hystricognathous and anomaluroid rodents. These degrees of complexity will be compared with those of their more ancient, coeval, or more recent counterparts. This study will further our understanding of the early evolutionary history of the incisor enamel microstructure within these two distinct groups of rodents from Africa.

Material and Methods

Several rodent incisors (complete or fragmentary) were collected from the coarse (mesh ≥ 2 mm) and thin (1 mm ≤ mesh < 2 mm) residues of screening of the DAK-Arg and DAK-Pto sediments (level C_2 [DAK C_2]). They correspond to upper (small radius of curvature) or lower (high radius of curvature) incisors of different sizes, showing a continuous range of width, primarily between 0.5 to 1.3 mm (Figs. 2 and 3). Although certain incisor specimens are complete and compatible in size with molars of different hystricognath and anomaluroid species from the same localities, a formal specific assignation of these incisors remains uncertain in the absence of well-preserved and complete mandibles and skulls having incisors associated with premolars and molars. Furthermore, several species of hystricognaths are very close in size (somewhat overlapping), a condition which makes difficult or even impossible a species attribution of the incisors. Two exceptions are the very large DAK-Pto-003 and DAK-Arg-073 upper incisors (width ≥ 1.6 mm), which can be confidently attributed to the largest rodent taxon recorded at DAK-Arg C_2 and DAK-Pto C_2 localities, the anomalurid *Paranomalurus riodeoroensis* (see Marivaux et al. 2017a). Otherwise, despite the lack of formal assignation for most of the specimens, we have nonetheless analyzed the enamel

microstructure of a set of incisors from each locality. We have selected 15 specimens (lower or upper incisor fragments) of different sizes in each locality. The specimens were embedded in artificial resin, then cut transversally in order to observe the enamel layer in cross section (Figs 2 and 3), and subsequently polished longitudinally. The polished sections were etched for 30 sec with phosphoric acid (H_3PO_4) at 37%, to make the enamel microstructural details visible. Each specimen was in fine examined by scanning electron microscope (SEM) at different magnifications (Figs. 4-8). The nomenclature of the enamel microstructure follows that of Koenigswald and Sander (1997) and Martin (1992, 1993). The measures carried out on the enamel layer observed in longitudinal section (Tables 1 and 2) follow those proposed by Martin (1992, 1993) and Boivin et al. (submitted). The datasets (SEM photographs) generated and analyzed during the current study are available from the corresponding author on reasonable request. In contrast, all prepared specimens during the current study are temporarily housed in the paleontological collections of the Université de Poitiers (Institut de Paléoprimatologie, Paléontologie Humaine : Évolution et Paléoenvironnements [iPHEP]). They will be subsequently housed permanently at the Université IBN Tofail, Kénitra (Morocco).

Results

Types of incisor enamel microstructures recorded and potential species attribution

Among the 30 incisors analyzed, only three specimens display an enamel characterized by uniserial Hunter-Schreger bands (HSBs). All the other specimens have an enamel

exhibiting multiserial HSBs (Tables 1 and 2). This low rate of recording of incisors with uniserial HSBs, corresponding to anomaluroid incisors, could have been in fact expected given the low number of cheek teeth (15) documenting the five anomaluroid species from DAK C_2. It was somewhat a chance to document at least five species with so little dental material (Marivaux et al. 2017a). As mentioned above, given the very large size (width ≥ 1.6 mm) of at least two incisors displaying an enamel with uniserial HSBs (DAK-Pto-003 and DAK-Arg-073; Tables 1 and 2; Fig. 4A-D), we can confidently attribute these two specimens to the largest taxon of the DAK C_2 rodent fauna, the anomalurid *Paranomalurus riodeoroensis*, the molars of which are compatible in size with these two incisors. The third incisor displaying an enamel with uniserial HSBs (DAK-Pto-043; Table 1; Fig. 4E-F) is a medium-sized specimen, and could either be attributed to the medium-sized nonanomalurid *Nonanomalurus parvus* or ?zegdoumyid *Dakhlamys ultimus*, the cheek teeth of these two anomaluroid taxa being similar in size (Marivaux et al. 2017a).

Regarding hystricognaths from DAK C_2, except for the tiny ?*Phiocricetomys* sp., which is known by a single lower molar, the six other species recorded are documented by much more dental material (see Marivaux et al. 2017b). This is consistent with the high rate of recording of incisors with multiserial HSBs. The dental material of *Mubhammys atlanticus* and *Phenacophiomys occidentalis* is particularly abundant. These two taxa are medium-sized species, *Phenacophiomys* being slightly larger than *Mubhammys*. Therefore, it might be expected that the few largest incisors (1.1 mm ≤ width ≤ 1.3 mm; Table 1 and 2) displaying an enamel characterized by multiserial HSBs (Figs. 5A-B, 7A-B and 8A-B) could have been those of *Phenacophiomys*. The abundant slightly smaller incisors (0.8 mm ≤ width ≤ 1.0 mm; Tables 1 and 2) could then have been those of *Mubhammys*. However, although abundant, the molars of *Mubhammys* are roughly similar in size to those of the two species of *Gaudeamus* (*Gaudeamus* cf. *G. hylaeus* and *Gaudeamus* cf. *G. aslius*) from DAK C_2, a dental size overlap

which then precludes any precise species attribution of these medium-sized incisors displaying an enamel with multiserial HSBs (Figs. 5C-F, 6A-B and 8C-F). The same is true regarding the smallest incisors (0.5 mm ≤ width ≤ 0.7 mm; Table 1 and 2) displaying an enamel with multiserial HSBs (Figs. 6C-F and 7C-F), which could either belong to the tiny species from DAK C_2, *Neophiomys minutus* or ?*Phenacophiomys* sp., or eventually to the slightly larger *Birkamys* aff. *B. korai*. It is worth noting that in the absence of complete mandibles and skulls having incisors associated with premolars and molars, our assessment of the taxonomic identification of the isolated incisors using for each enamel category ('uniserial HSBs-anomaluroids' and 'multiserial HSBs-hystricognaths'), the criterion of size compatibility between incisors and cheek teeth remains only tentative.

Incisor enamel with uniserial HSBs

We have sampled only three upper incisors (no lower incisor) displaying an enamel with uniserial HSBs. Among them, the two largest specimens (DAK-Pto-003 and DAK-Arg-073; Tables 1 and 2; Fig. 4A-D) exhibit roughly similar microstructural arrangements. Despite a difference in the total enamel thickness between the two incisors (enamel layer slightly thinner in DAK-Arg-073, but that specimen is also slightly smaller than DAK-Pto-003), both specimens are characterized by a strong development (i.e., thick) of the Portio externa (PE). The Portio interna (PI) of their enamel layer consists of decussating HSBs, among which about 80% display one prism per band, and punctually (not regularly) two prisms per band. The HSBs are straight and faintly inclined (max. 10°). The prisms are strongly flattened, thereby appearing oval and inclined in cross section. The inter-prismatic matrix (IPM) in the PI is thin and does not form a sheath surrounding the prisms. The IPM crystallites rather form

thin sheets that run nearly parallel to the prism direction and anastomose continuously between the prisms. This generates an IPM sheet of transition between two adjacent decussating HSBs. Such an IPM crystallite arrangement in PI associated with the occasional presence of HSBs having two prisms per band testify of an early stage toward the achievement of a fully uniserial condition (Korvenkontio 1934; Martin 1993, 1997).

The third upper incisor displaying an enamel with uniserial HSBs is a medium-sized specimen (DAK-Pto-043; Table 1; Fig. 4E-F). As the two other large upper incisors described above, the enamel layer of this specimen is moderately thin (compared with large-, medium-, or small-sized incisors with an enamel characterized by multiserial HSBs) and with a thick PE. The latter is however slightly thinner than in the two other anomaluroid incisors. In the PI of the enamel layer of DAK-Pto-043, 100% of the decussating HSBs have only one prism per band. The HSBs are also much more inclined (~ 56°) than in the enamel of the two other incisors. The prisms are less flattened, appearing round or slightly oval in cross section. The IPM crystallites in the PI form thin sheets that run nearly parallel to the prism direction, without frequent anastomoses. Such an IPM crystallite arrangement in PI associated with HSBs having only one-prism layers, testify of an early stage of the uniserial condition.

Incisor enamel with multiserial HSBs

Of the 30 incisor fragments of different sizes selected from the two localities of the Dakhla level C_2 (DAK-Pto and DAK-Arg), we have in fact primarily sampled upper and lower incisors of hystricognaths, inasmuch as 27 specimens exhibit an enamel with multiserial HSBs (Tables 1 and 2). Whatever the size (large-sized [1.1 mm ≤ width ≤ 1.3 mm], medium-sized [0.8 mm ≤ width ≤ 1.0 mm], or small-sized [0.5 mm ≤ width ≤ 0.7 mm] specimens) or

the jaw position (upper or lower) of the incisors, we do not observe strong variation in the enamel crystallite arrangements. The majority of incisors displays an enamel with multiserial HSBs, the IPM crystallites of which appear as thin sheets that anastomose regularly, and their direction form an acute angle to the prism direction. Following Martin (1992, 1993, 1994, 1997, 2007) (but also Vieytes 2003; Vucetich and Vieytes 2006), this kind of crystallite arrangement typifies the subtype 2 of multiserial HSBs. Despite that unique subtype record, we observe nonetheless some variations across incisors, principally in the thickness of the enamel layer, in the value of the acute angle (wide amplitude) formed between the direction of the prism crystallites and those of the IPM sheets, and to a lesser extent, in the number of prisms per HSBs, the inclination of the HSBs, and in the frequency of the IPM sheet anastomoses (Tables 1 and 2). Therefore, instead of describing exhaustively the enamel microstructure for each incisor sampled (all exhibiting a subtype 2 of multiserial HSBs), here after we focus on the main microstructural characters that can differ between incisors of different sizes and between upper and lower incisors (of similar size).

Large-sized incisors: Among lower incisors of similar size (equal width), the enamel thickness strongly varies (+ 60%; e.g., DAK-Pto-042 vs DAK-Pto-037; Table 1; Fig. 5A-B). Such a marked difference in enamel thickness could indicate the presence of distinct species equivalent in size. However, despite this thickness distinction, the crystallite arrangements are roughly similar, notably regarding the IPM configuration, which shows a comparable range in the values of the acute angle formed between the IPM sheets and the prism long axes. The unique upper incisor analyzed for this size category (DAK-Arg-074; Table 2; Fig. 8A-B) display a thick enamel layer, similar to that of the lower DAK-Pto-037 incisor (Table 2; Fig. 5A-B). In contrast, that upper incisor displays an enamel with thicker HSBs, having 4-5 prisms per band, contra 3-4 prisms per band in the other large specimens. In this upper

incisor, the value of the acute angle between the crystallites of IPM and the prism direction is also often less marked (Table 2; Fig. 8B).

Medium-sized incisors: This size category also exhibits a wide spectrum of enamel thickness among and within the lower and upper specimens. Two upper incisors (DAK-Arg-076 and DAK-Arg-085; Table 2; Fig. 8E-F) display particularly thick HSBs, including 5-6 prisms per band, and a moderate value of the acute angle between the crystallites of IPM and those of the prisms. Other upper incisors of this size category have rather 3-4 prisms per HSB but similar values of the IPM/prism crystallite angles (Tables 1 and 2). Lower incisors display also 3-4 prisms per HSB, and generally slightly higher values of the IPM/prism crystallite angles. Practically all specimens display prisms of transitional zone between two adjacent HSBs. One upper incisor (DAK-Pto-038; Table 1; Fig. 6A-B), among the smallest one of this size category (i.e., width = 0.8 mm), exhibits prisms having a section appearing more rounded (circular) than that observed in the other upper or lower specimens (prisms being oval to flattened in section). The IPM crystallites deviate only by 23° from those of the prisms, and anastomose very frequently (very regularly), more than on the other specimens. However, the IPM crystallites do not form a sheath-like IPM (as the condition describing the subtype 1 of multiserial HSBs), but form sheets. Given the latter characteristics, this specimen could illustrate a case of transitional subtype 1-2 of multiserial HSBs.

Small-sized incisors: We have analyzed the enamel microstructure of several lower and upper incisors of this size category (Tables 1 and 2; Figs. 6C-F and 7C-F). Practically all specimens have 3-4 prisms per HSB (rarely up to 5 prisms per band), a similar HSB inclination, no prisms of transitional zone between two adjacent decussating HSBs, and a

relatively similar enamel thickness, except for one specimen (DAK-Arg-079; Table 2; not figured). The latter, an upper incisor, indeed shows a markedly thinner enamel layer than that of the other upper and lower incisors of similar size (width = 0.7 mm). Within this size category, two upper incisors (DAK-Pto-046 and DAK-Pto-050; Table 1; Fig. 6C-D) have moderately low values (~ 25°) of the angle formed between the crystallites of IPM and those of the prisms. On these two specimens, the sheets of IPM also anastomose very frequently, nearly forming a sheath-like IPM arrangement (Fig. 6D). In contrast, some incisors of this size category, notably the lower incisors (e.g., DAK-Arg-077 [Fig. 7C-D], DAK-Arg-082 [Fig. 7E-F], and DAK-Pto-049) exhibit markedly higher values of the IPM/prism crystallite angles (50° up to 60°; Tables 1 and 2), with less frequent to rare anastomoses of the IPM sheets. With such an IPM arrangement, the latter incisors illustrate an enamel microstructure characterized by an advanced subtype 2 of multiserial HSBs.

Discussion and Conclusion

These earliest Oligocene estuarine deposits from Dakhla (DAK C_2) yield the only Paleogene rodent assemblage from the Atlantic margin of North Africa (Atlantic Sahara). The great rodent diversity recorded in that area, associating in sympatry at least seven hystricognaths and five anomaluroids was somewhat unexpected given the unfavorable global climatic conditions characterizing this time window (i.e., global cooling recorded at the Eocene/Oligocene transition). Such a rodent diversity from DAK C_2, including several arboreal species, rather indicates that this tropical region of North Africa was seemingly less affected by these climatic changes (Marivaux et al. 2017a,b). This new northwestern African fauna hence represents a remarkable snapshot regarding the paleodiversity of rodents at that

time, and balances the early Oligocene rodent fossil record of North Africa, which was so far only documented by fossil assemblages from northern and northeastern Africa (Libya, Egypt) and from Arabia (Dhofar in Oman). Wet-screening of the sediments of the two rodent-bearing localities from DAK C_2 has allowed collecting many isolated cheek teeth but also many fragments of rodent incisors. Despite these fragments are isolated, and as such not formally (or firmly) attributed to a given species, we thought it worthwhile to analyze the enamel microstructure of several specimens of different sizes in order to have, for the first time, an overview of the enamel evolutionary degrees recorded for an African rodent community of that age. Indeed, only few analyses of the rodent incisor enamel microstructure have been carried out for African fossil rodents. For the Oligocene of Africa, the incisor enamel microstructure is only documented for *Phiomys andrewsi*, *Metaphiomys schaubi*, *Gaudeamus aegyptius* (see Martin 1992), *G. lavocati* (Martin in Coster et al. 2010) and *Turkanamys hexalophus* (see Marivaux et al. 2012) (ESM 1). These taxa occur in stratigraphic levels more recent than DAK C_2 (for a review, see Marivaux et al. 2017b: fig. 10). The latest Eocene L-41 locality of the Fayum, Egypt, very close in age to DAK C_2, and that yields a great hystricognath diversity (Holroyd 1994; Sallam et al. 2011, 2012; Sallam and Seiffert 2016), has not hitherto been the subject of incisor enamel microstructure analyses. The same is true for the BQ-2 locality (Fayum) dating from the early late Eocene, the Dur at-Talah localities (Libya) dating from the late Eocene, or for the Taqah locality (Oman) dating from the early Oligocene, localities which yield sympatric anomaluroid and hystricognathous rodents (Thomas et al. 1989, 1992; Sallam et al. 2009, 2010a,b; Jaeger et al. 2010; Coster et al. 2015). The enamel microstructure for Eocene African rodents is only documented for the late middle to early late Eocene hystricognath *Protophiomys tunisiensis* (Tunisia; see Marivaux et al. 2014) and ?*P. algeriensis* (Algeria; see Coiffait et al. 1984; Martin 1992, 1993) (see ESM 1), and for the late early to early middle Eocene zegdoumyid anomaluroids (Algeria and Tunisia;

Martin 1993; Marivaux et al. 2011, 2015) and early late Eocene nementchamyid anomaluroids (Algeria; Martin 1993) (see ESM 2). With the study of the incisor enamel of the rodent fauna from Dakhla (DAK C_2), we then contribute to a better knowledge of the diversity and evolutionary degree of the enamel microtextural pattern developed at that time for the two emblematic African rodent groups: anomaluroids and hystricognaths.

The numerous works of Martin (e.g., 1992, 1993, 1994, 1995, 1997) concerning the analysis of the incisor enamel microstructure in rodents, have shown that all hystricognaths display an enamel characterized by multiserial HSBs (ESM 1), whereas anomaluroids exhibit an enamel incisor with uniserial HSBs (or transitional pauciserial/uniserial HSBs for the stem groups; ESM 2). These clearly distinct enamel patterns allow therefore for a proper supra-familial attribution of the isolated incisors from DAK C_2. In contrast, their generic or specific attributions remain much more delicate in the absence of preserved incisor-premolar-molar association, and the criterion of size compatibility between incisors and cheek teeth in each enamel category remains only tentative (see results). Despite the large number of incisors sampled for this study, we found only three incisors having an enamel with uniserial HSBs. This small number of anomaluroid incisors sampled is consistent with the small number of anomaluroid cheek teeth recovered in DAK-Arg C_2 and DAK-Pto C_2, and documenting the five species (Marivaux et al. 2017a). Two large incisors are likely attributable to *Paranomalurus riodeoroensis*, the largest rodent from DAK C_2. The enamel microstructure of these two incisors is characterized by a thinning of the HSBs, with generally a single flattened prism per band, but also occasionally two prisms per band, and a thin IPM that runs parallel to the prism direction, thereby typifying an early stage toward the achievement of a fully uniserial condition. The third anomaluroid incisor (slightly smaller in size than the two others) has an enamel displaying 100% of uniserial HSBs (no double-layered HSBs observed), but with a similar thin IPM sheet arrangement (i.e., parallel to the prism direction) and with prism

having a round section, thereby testifying of an early stage of the uniserial condition. The incisor enamel microstructure of modern anomaluroids is only documented by the genus *Anomalurus* (Anomalurinae, Anomaluridae). The incisor enamel of this taxon primarily shows single flattened prism layers, but also, only rarely, double-layered HSBs, and a thin IPM that runs parallel to the prism direction (Martin 1993, 1997), an enamel microstructural pattern that is in fact strongly reminiscent to that observed in *Paranomalurus riodeoroensis* (Anomalurinae) from Dakhla. Unfortunately, nothing is known regarding the incisor enamel microstructure of the other modern anomaluroids, *Anomalurops* (Anomalurinae, Anomaluridae), *Idiurus* (Idiurinae, Anomaluridae) and *Zenkerella* (Zenkerellidae), or of the Miocene taxa such as the different species of *Paranomalurus* (*P. walkeri*, *P. bishopi*; Anomalurinae, Anomaluridae), and *Nonanomalurus soniae* (Nonanomaluridae). This lack of enamel description for Miocene and modern anomaluroids limits *i)* our comparisons and therefore the precise assessment of the enamel evolutionary degree observed in anomaluroids from Dakhla, and *ii)* our understanding of the evolutionary trends of the enamel microstructure in this rodent group. The incisor enamel microstructure is somewhat better documented for stem anomaluroids, notably for the Eocene zegdoumyids and nementchamyids (Martin 1993; Marivaux et al. 2005, 2011) (ESM 2). These two groups have an incisor enamel showing the tendency towards a thinning of the HSBs (one or one-two prisms per band), a trend observed as early as the late early Eocene (in zegdoumyids), but the IPM crystallite arrangement in that enamel is not as advanced as in the anomalurine enamel incisors from Dakhla. In zegdoumyids and nementchamyids, the IPM is indeed thicker, parallel to the prism direction, and generally forms a sheath surrounding the prisms (not appearing as thin sheets). Such an IPM arrangement typifies an enamel transitional from the primitive pauciserial to the uniserial condition (Martin 1993; Marivaux et al. 2005, 2011).

The other DAK C_2 sampled incisors display an enamel with multiserial HSBs. Despite the large number of incisors with this enamel type, we recorded primarily an IPM crystallite arrangement describing the subtype 2 of multiserial HSBs (Martin 1992, 1993, 1994, 1997; Vieytes 2003). However, we observed many microstructural variations across incisors (i.e., differences in the degree of crystallite arrangements), likely reflecting different species. We recorded indeed a wide amplitude in the angle (acute) formed between the crystallites of IPM and those of the prisms, some variations in the frequency of the IPM sheet anastomoses, in the number of prisms per HSBs, and variations in the inclination of the HSBs (Tables 1 and 2). The thickness of the enamel layer also strongly varies across incisors of different sizes and within a size category. Only two incisors show an enamel with an IPM crystallite arrangement that describes a case of transitional subtype 1-2 of multiserial HSBs, and three others have an enamel characterized by an advanced subtype 2 of multiserial HSBs (see results). The subtype 2 of multiserial enamel is widespread among modern and extinct New World hystricognaths (i.e., caviomorphs, notably chinchilloids, cavioids, and erethizontoids, with the exception of most octodontoids; Martin 1992, 1993, 1994; 2004, 2005; Vieytes 2003; Vucetich and Vieytes 2006; Vucetich et al. 2010; for a review see Boivin et al. submitted), among early Old Word hystricognaths (e.g., Asian tsaganomyids, South Asian baluchimyines, early African protophiomyines, phiomyids, and gaudeamurids; Martin 1992; Marivaux 2000; Marivaux et al. 2000, 2012; Martin in Coster et al. 2010; see ESM 1), but also in Asian "ctenodactyloids" (e.g., early diatomyids and early ctenodactylids; Martin 1992, 1995, 2007; Marivaux et al. 2004; see ESM 1). It is worth noting that from the large set of incisor fragments analyzed from DAK C_2, we did not record any enamel documenting a subtype 1 of multiserial HSBs, as that observed in the oldest hystricognath rodent to be known in Africa thus far (*Protophiomys tunisiensis*, 39.5 Ma; see Marivaux et al. 2014), but also in certain early Oligocene baluchimyine hystricognaths from South Asia (Martin 1992, 1995), in the middle Eocene

tamquammyid ctenodactyloids from Mongolia (Martin 1993, 1995, 2007), and in the early Miocene diamantomyid taxon (*Diamantomys*; hystricognaths) from Kenya (Martin 1992) (ESM 1). The subtype 1 is also characteristic of the incisor enamel of modern hystricids (Martin 1992), and it is particularly widespread among several extinct and extant caviomorphs, notably in erethizontoids, cavioids, and chinchillids (Martin 1992, 2004, 2005; Vieytes 2003; for a review see Boivin et al. submitted). Also, we did not record in DAK C_2 any enamel documenting the transitional subtype 2-3 and the subtype 3 of multiserial HSBs, as that characterizing some more recent and evolutionarily advanced phiomorphs (ESM 1), such as *Metaphiomys schaubi* (early Oligocene) or *Paraphiomys pigotti* (early Miocene). All modern phiomorphs (i.e., Thryonomyoidea; ESM 1) have an incisor enamel characterized either by the subtype 2-3 of multiserial HSBs (Thryonomyidae and Bathyergidae) or by the subtype 3 of multiserial HSBs (Petromuridae). The latter enamel microstructure also characterizes incisors of modern and most of extinct South American octodontoid caviomorphs (Martin 1992, 1994, 2005; Vieytes 2003; Vieytes et al. 2007; Morgan et al. 2017; for a review see Boivin et al. submitted), as well as some Miocene and modern "ctenodactyloids" (ctenodactylids and diatomyids; Martin 1992, 1995; Dawson et al. 2006) (ESM 1). The subtype 3 of multiserial HSBs is characterized by IPM crystallites running at a right angle to those of the prisms (plate-like IPM with a few or no anastomoses). Given that an increasing angulation of the IPM sheets is considered as strengthening the enamel in the third dimensions, multiserial HSBs with rectangular IPM (subtype 3) provide to the incisor enamel a better resistance to the crack propagations (Martin 1992, 1993, 1994, 1997, 2007). On the basis of this biomechanical consideration and the stratigraphic occurrences of taxa, the subtype 3 is considered as the most derived and specialized multiserial condition. Accordingly, considering the IPM arrangement, the subtype 1 is the most primitive (and the less resistant) condition of multiserial HSBs, and the subtype 2 is intermediary in terms of

resistance and evolutionary degree, between the subtypes 1 and 3 (Martin 1992, 1993, 1994, 1997). The subtypes 1 and 2 (and the transitional subtype 1-2) are therefore preserved in several modern hystricognaths, and the subtype 3 (and the transitional subtype 2-3) seems to have been acquired iteratively in several extinct and extant groups (Martin 1992, 1994; see also Vucetich and Vieytes 2006; Boivin et al. submitted).

In DAK C_2, dating from the earliest Oligocene, we record almost exclusively the intermediary subtype 2 and no subtype 1 and 3 (or 2-3) of multiserial HSBs. Given the absence of the subtypes 2-3 and 3 in DAK C_2, we might then question whether African hystricognathous rodents had already achieved the most resistant multiserial HSBs at that time. But, the possibility exists that this unique enamel subtype 2 sampling from Dakhla is the result of a taphonomic bias, or that taxa displaying the subtypes 2-3 or 3 of multiserial HSBs were not present in the westernmost part of Africa at that time. A fully achieved subtype 3 of multiserial HSBs is observed shortly after the DAK C_2 record, notably in the early Oligocene localities of the Fayum in Egypt, with *Metaphiomys schaubi* (Martin 1992). Recent analyses of the enamel microstructure of Eocene and Oligocene rodent incisors from Peruvian Amazonia (Boivin et al. submitted) have shown that the subtypes 2-3 and 3 of multiserial HSBs are only recorded from early Oligocene localities (i.e., Shapara and Santa Rosa; see also Martin 2004, 2005 for Santa Rosa, the age of which is uncertain: ?latest Eocene/early Oligocene), and not in older Eocene localities (Contamana), where only the subtypes 1 and 2 are recorded. Boivin et al. (submitted) have suggested that the derived subtypes 2-3 and 3 conditions were secondarily but rapidly achieved in caviomorphs, "and seemingly evolved iteratively but only in the octodontoid clade" (see also Vucetich and Vieytes 2006), the subtypes 1 and 2 being "conserved in most of caviomorph superfamilies through time" (Boivin et al. submitted). For Ctenohystrica in general, it would be then interesting to identify the ecological (and perhaps genetic?) and paleoenvironmental factors, that have driven the

achievement and selection of more resistant incisor enamel microstructures (subtypes 2-3 and 3) in certain groups only, while other taxa, in seemingly similar environments, conserved less resistant microstructures (subtypes 1, 2, or 1-2) through time. For Africa, we might question whether the drier, cooler climatic regime of the early Oligocene, having probably increased the fragmentation and opening of habitats (with more abrasive and harder food items), have played a role in the selection of taxa having acquired a more resistant incisor enamel in these region of North Africa. But a similar scenario could be also advocated for explaining the Oligocene achievement of a subtype 3 of multiserial HSBs in Old World "ctenodactyloids" (i.e., ctenodactylids and diatomyids) and in some New World hystricognaths (i.e., octodontoids), inasmuch as the climatic deterioration of the early Oligocene was recorded at the global scale (e.g., Coxall et al. 2005; Lear et al. 2008; Zachos et al. 2008; Hren et al. 2013; Tramoy et al. 2016). Only a broader analysis of the incisor enamel microstructure in hystricognathous rodents (and more widely Ctenohystrica) documenting the late Eocene – early Oligocene time interval would allow to assess the timing of achievement of the subtypes 2-3 and 3 of multiserial HSBs, and the possible relationships with the paleoenvironmental changes.

Acknowledgments We are indebted to Henri Cappetta (ISE-M), Sébastien Enault (ISE-M), Jérôme Surault (iPHEP), Imad Elkati, Abdallah Tarmidi, Mbarek Fouadasi, and the local people of Dakhla for their assistance during the successive field seasons (2009-2017). We are grateful to Sandra Unal (ISE-M), Suzanne Jiquel (ISE-M), Bernard Marandat (ISE-M), Théo Mancuso (Université de Montpellier), and Jérôme Surault (iPHEP) for their contribution in the picking of the fossil specimens from Porto Rico (Pto) and El Argoub (Arg). We warmly thank Thomas Martin (Universität Bonn, Germany) for his useful advice regarding the enamel microstructure of rodent incisors. Many thanks to Chantal Cazevieille and Alicia Caballero-

Megido (Montpellier RIO Imaging [MRI] and Institute for Neurosciences Montpellier [INM], France) for access to scanning electron microscope (SEM) facilities. We also thank the two anonymous external reviewers, who provided formal reviews of this manuscript that enhanced the final version. This research was supported by the French ANR-ERC PALASIAFRICA (ANR-08-JCJC-0017) and ANR EVAH (ANR-09-BLAN-0238) programs, the MEDYNA program (Maghreb-Eu research staff exchange on geoDYnamics, geohazards and applied geology in Northwest Africa; FP7, PIRSES-GA-2013-612572), and by the ISE-M UMR CNRS/UM/IRD/EPHE 5554 (*Laboratoire de Paléontologie*) and iPHEP UMR CNRS 7262. This is ISE-M publication 2018-0XX SUD.

References

Adnet S, Cappetta H, Enault S, Benammi M, Marivaux L, Tabuce R, Saddiqi O, Baidder L, Benammi M (2017) The late Eocene/Oligocene elasmobranch fauna of the Samlat Formation in Dakhla, Morocco: a mirror of the coeval World Heritage sites of Egypt. The First West African Craton and Margins International Workshop (WACMA1), Dakhla, Morocco. Abstract Volume:81-82

Benammi M, Adnet S, Marivaux L, Yans J, Noiret C, Tabuce R, Surault J, El Kati I, Enault S, Baidder L, Saddiqi O, Benammi M (2017) Geology, biostratigraphy and carbon isotope chemostratigraphy of the Paleogene fossil-bearing Dakhla sections, southwestern Moroccan Sahara. Geol Mag in press. doi: 10.1017/S0016756817000851

Berggren WA, Prothero DR (1992) Eocene-Oligocene Climatic and Biotic Evolution: An Overview. Princeton University Press, Princeton

Boivin M, Marivaux L, Salas-Gismondi R, Vieytes EC, Antoine P-O (201X) Incisor enamel microstructure of Paleogene caviomorph rodents from Contamana and Shapaja (Peruvian Amazonia). J Mammal Evol submitted

Coiffait PE, Coiffait B, Jaeger J-J, Mahboubi M (1984) Un nouveau gisement à mammifères fossiles d'âge Éocène supérieur sur le versant Sud des Nementcha (Algérie orientale) : découverte des plus anciens rongeurs d'Afrique. C R Acad Sc Paris 13:893-898

Coster P, Benammi M, Lazzari V, Billet G, Martin T, Salem M, Bilal AA, Chaimanee Y, Schuster M, Valentin X, Brunet M, Jaeger J-J (2010) *Gaudeamus lavocati* sp. nov. (Rodentia, Hystricognathi) from the early Oligocene of Zallah, Libya: first African caviomorph? Naturwissenschaften 97(8):697-706

Coster P, Benammi M, Salem M, Bilal AA, Chaimanee Y, Valentin X, Brunet M, Jaeger J-J (2012) New hystricognath rodents from the lower Oligocene of central Libya (Zallah Oasis, Sahara desert): systematic, phylogeny and biochronologic implications. Ann Carnegie Mus 80:239-259

Coster PMC, Beard KC, Salem MJ, Chaimanee Y, Jaeger J-J (2015) New fossils from the Paleogene of central Libya illuminate the evolutionary history of endemic African anomaluroid rodents. Frontiers Earth Sci 3(56):1-15

Coxall HK, Wilson P, Palike H, Lear C, Backman J (2005) Rapid stepwise onset of Antarctic glaciation and deeper calcite compensation in the Pacific Ocean. Nature 433:53-57

Dawson MR, Marivaux L, Li C-K, Beard KC, Métais G (2006) *Laonastes* and the "lazarus effect" in Recent mammals. Science 311:1456-1458

Holroyd PA (1994) An examination of dispersal origins for Fayum mammals. PhDissertation, Duke University, Durham

Hren MT, Sheldon ND, Grimes ST, Collinson ME, Hooker JJ, Bugler M, Lohmann KC (2013) Terrestrial cooling in Northern Europe during the Eocene-Oligocene transition. Proc Natl Acad Sci USA 110:7562-7567

Jaeger J-J, Marivaux L, Salem M, Bilal AA, Chaimanee Y, Marandat B, Valentin X, Duringer P, Schuster M, Benammi M, Métais E, Brunet M (2010) New rodent assemblages from the Eocene Dur at-Talah escarpment (Sahara of Central Libya): systematic, biochronologic and paleobiogeographic implications. Zool J Linn Soc 160:195-213

Koenigswald Wv, Sander PM (1997) Glossary of terms used for enamel microstructures. In: Koenigswald Wv, Sander PM (eds) Tooth Enamel Microstructure. Balkema, Rotterdam, pp 267-280

Korvenkontio VA (1934) Mikroskopische Untersuchungen an Nagerincisiven unter Hinweis auf die Schmelzstruktur der Backenzähne. Ann Zoo Soc Zool – Bota Fennicae Vanamo 2:1-274

Lear CH, Bailey TR, Pearson PN, Coxall HK, Rosenthal Y (2008) Cooling and ice growth across the Eocene-Oligocene transition. Geology 36:251-254

Marivaux L (2000) Les rongeurs de l'Oligocène des Collines Bugti (Balouchistan, Pakistan) : nouvelles données sur la phylogénie des rongeurs paléogènes, implications biochronologiques et paléobiogéographiques. PhDissertation, Université Montpellier II, Sciences et Techniques du Languedoc

Marivaux L, Adaci M, Bensalah M, Gomes Rodrigues H, Hautier L, Mahboubi M, Mebrouk F, Tabuce R, Vianey-Liaud M (2011) Zegdoumyidae (Rodentia, Mammalia), stem anomaluroid rodents from the early to middle Eocene of Algeria (Gour Lazib, western Sahara): new dental evidence. J Syst Palaeontol 9(4):563-588

Marivaux L, Adnet S, Benammi M, Tabuce R, Benammi M (2017a) Anomaluroid rodents from the earliest Oligocene of Dakhla, Morocco, reveal the long-lived and morphologically conservative pattern of the Anomaluridae and Nonanomaluridae during the Tertiary in Africa. J Syst Palaeontol 15(7):539-569

Marivaux L, Adnet S, Benammi M, Tabuce R, Yans J, Benammi M (2017b) Earliest Oligocene hystricognathous rodents from the Atlantic margin of northwestern Saharan Africa (Dakhla, Morocco): systematic, paleobiogeographical and paleoenvironmental implications. J Vertebr Paleontol 37(5):e1357567; doi: 10.1080/02724634.2017.1357567

Marivaux L, Benammi M, Ducrocq S, Jaeger J-J, Chaimanee Y (2000) A new baluchimyine rodent from the late Eocene of the Krabi Basin (Thailand): paleobiogeographic and biochronologic implications. C R Acad Sc Paris 331(6):427-433

Marivaux L, Chaimanee Y, Yamee C, Srisuk P, Jaeger J-J (2004) Discovery of *Fallomus ladakhensis* Nanda & Sahni, 1998 (Rodentia, Diatomyidae) in the lignites of Nong Ya Plong (Phetchaburi Province, Thailand): systematic, biochronologic and paleoenvironmental implications. Geodiversitas 26(3):493-507

Marivaux L, Ducrocq S, Jaeger J-J, Marandat B, Sudre J, Chaimanee Y, Tun ST, Htoon W, Soe AN (2005) New remains of *Pondaungimys anomaluropsis* (Rodentia, Anomaluroidea) from the latest middle Eocene Pondaung Formation of Central Myanmar. J Vertebr Paleontol 25(1):214-227

Marivaux L, Essid EM, Marzougui W, Khayati Ammar H, Adnet S, Marandat B, Merzeraud G, Tabuce R, Vianey-Liaud M (2014) A new and primitive species of *Protophiomys* (Rodentia, Hystricognathi) from the late middle Eocene of Djebel el Kébar, central Tunisia. Palaeovertebrata 38(1-e2):1-17

Marivaux L, Essid EM, Marzougui W, Khayati Ammar H, Merzeraud G, Tabuce R, Vianey-Liaud M (2015) The early evolutionary history of anomaluroid rodents in Africa: new dental remains of a zegdoumyid (Zegdoumyidae, Anomaluroidea) from the Eocene of Tunisia. Zool Scrip 44(2):117-134

Marivaux L, Lihoreau F, Manthi KF, Ducrocq R (2012) A new basal phiomorph (Rodentia, Hystricognathi) from the late Oligocene of Lokone (Turkana Basin, Kenya). J Vertebr Paleontol 32(3):646-657

Martin T (1992) Schmelzmikrostruktur in den Inzisiven alt und neuweltlicher hystricognather Nagetiere. Palaeovertebrata Mém extra:1-168

Martin T (1993) Early rodent incisor enamel evolution: phylogenetic implications. J Mammal Evol 1(4):227-254

Martin T (1994) African origin of caviomorph rodents is indicated by incisor enamel microstructure. Paleobiology 20(1):5-13

Martin T (1995) Incisor enamel microstructure and phylogenetic interrelationships of Pedetidae and Ctenodactyloidea (Rodentia). Berliner Geowiss Abh 16:693-707

Martin T (1997) Incisor enamel microstructure and systematics in rodents. In: Koenigswald Wv, Sander PM (eds) Tooth Enamel Microstructure. Balkema, Rotterdam, pp 163-175

Martin T (2004) Incisor enamel microstructure of South America's earliest rodents: implications for caviomorph origin and diversification. In: Campbell KE (ed) The Paleogene Mammalian Fauna of Santa Rosa, Amazonian Peru. Nat Hist Mus Los Angeles County, Los Angeles, pp 131-140

Martin T (2005) Incisor schmelzmuster diversity in South America's oldest rodent fauna and early caviomorph history. J Mammal Evol 12(3/4):405-417

Martin T (2007) Incisor enamel microstructure and the concept of Sciuravida. In: Beard KC, Luo Z-X (eds) Mammalian Paleontology on a Global Stage: Papers in Honor of Mary R. Dawson. Bull Carnegie Mus Nat Hist 39:127-140

Morgan CC, Verzi DH, Olivares AI, Vieytes EC (2017) Craniodental and forelimb specializations for digging in the South American subterranean rodent *Ctenomys* (Hystricomorpha, Ctenomyidae). Mammal Biol 87:118-124

Noiret C, Benammi M, Adnet S, Enault S, Marivaux L, Tabuce R, Surault J, Baidder L, Saddiqi O, El Kati I, Benammi M, Yans J (2017) Carbon isotope chemostratigraphy on organics (δ13Corg): a powerful tool to refine the Paleogene age of the fossil-bearing levels in the Dakhla area (southwestern Moroccan Sahara). The First West African Craton and Margins International Workshop (WACMA1), Dakhla, Morocco. Abstract Volume:79-80.

Sallam HM, Seiffert ER (2016) New phiomorph rodents from the latest Eocene of Egypt, and the impact of Bayesian "clock"-based phylogenetic methods on estimates of basal hystricognath relationships and biochronology. PeerJ 4:e1717:1-53

Sallam HM, Seiffert ER, Simons EL (2010a) A highly derived anomalurid rodent from the earliest late Eocene of Egypt. Palaeontology 53(4):803-813

Sallam HM, Seiffert ER, Simons EL (2011) Craniodental morphology and systematics of a new family of hystricognathous rodents (Gaudeamuridae) from the late Eocene and early Oligocene of Egypt. PLoS One 6(2):1-29

Sallam HM, Seiffert ER, Simons EL (2012) A basal phiomorph (Rodentia, Hystricognathi) from the late Eocene of the Fayum Depression, Egypt. Swiss J Palaeontol 131(2):283-301

Sallam HM, Seiffert ER, Simons EL, Brindley C (2010b) A large-bodied anomaluroid rodent from the earliest late Eocene of Egypt: phylogenetic and biogeographic implications. J Vertebr Paleontol 30(5):1579-1593

Sallam HM, Seiffert ER, Steiper ME, Simons EL (2009) Fossil and molecular evidence constrain scenarios for the early evolutionary and biogeographic history of hystricognathous rodents. Proc Natl Acad Sci USA 106:16722-16727

Thomas H, Roger J, Sen S, Al-Sulaimani Z (1992) Early Oligocene vertebrates from Dhofar (Sultanate of Oman). In: Sadek A (ed) Geology of the Arab World. Cairo University, Cairo, pp 283-293

Thomas H, Roger S, Sen S, Bourdillon-de-Grissac C, Al-Sulaimani Z (1989) Découverte de vertébrés fossiles dans l'Oligocène inférieur du Dhofar (Sultanat d'Oman). Geobios 22(1):101-120

Tramoy R, Salpin M, Schnyder J, Person A, Sebilo M, Yans J, Vaury V, Fozzani J, Bauer H (2016) Stepwise palaeoclimate change across the Eocene–Oligocene transition recorded in continental NW Europe by mineralogical assemblages and $\delta^{15}N_{org}$ (Rennes Basin, France). Terra Nova 28(3):212-220

Vieytes EC (2003) Microestructura del esmalte de roedores Hystricognathi sudamericanos fósiles y vivientes: significado morfofuncional y filogenético. PhDissertation, Universidad Nacional de La Plata, La Plata

Vieytes EC, Morgan CC, Verzi DH (2007) Adaptive diversity of incisor enamel microstructure in South American burrowing rodents (family Ctenomyidae, Caviomorpha). J Anat 211(3):296-302

Vucetich MG, Vieytes EC (2006) A middle Miocene primitive octodontoid rodent and its bearing on the early evolutionary history of the Octodontoidea. Palaeontographica Abt A 277:81–91

Vucetich MG, Vieytes EC, Pérez ME, Carlini AA (2010) The rodents from La Cantera and the early evolution of caviomorphs in South America In: Madden RH, Carlini AA, Vucetich MG, Kay RF (eds) The Paleontology of Gran Barranca, Evolution and Environmental Change through the Middle Cenozoic of Patagonia. Cambridge University Press, Cambridge, pp 189–201

Wood AE (1968) Part II: The African Oligocene Rodentia. In: Remington JE (Ed) Early Cenozoic Mammalian Faunas Fayum Province, Egypt. Peabody Mus Nat Hist Yale Univ, New Haven, pp 23-105

Zachos JC, Dickens GR, Zeebe RE (2008) An early Cenozoic perspective on greenhouse warming and carbon-cycle dynamics. Nature 451: 279–283

Figure captions

Fig. 1 Geographic locations of the Dakhla peninsula, northwestern Africa (Atlantic Sahara), and of the fossil rodent-bearing localities. The geological outcrops of interest (El Argoub [Arg] and Porto Rico [Pto]) are exposed on the mainland shoreline of the *Rio de Oro* inlet, east of the Dakhla peninsula (photographs by L. Marivaux). The rodent-bearing localities, El Argoub level C_2 (DAK-Arg C_2) and Porto Rico level C_2 (DAK-Pto C_2), are situated directly southeast of the Dakhla city. On the two photographs, the dashed white lines indicate the fossiliferous level C_2, which consists of a ca. 30 cm thick sandy and unconsolidated microconglomerate.

Fig. 2 Incisor cross-sections of Dakhla C_2 rodents from Porto Rico. **a**, DAK-Pto-043. **b**, DAK-Pto-037. **c**, DAK-Pto-038. **d**, DAK-Pto-039. **e**, DAK-Pto-044. **f**, DAK-Pto-041. **g**, DAK-Pto-042. **h**, DAK-Pto-046. **i**, DAK-Pto-048. **j**, DAK-Pto-040. **k**, DAK-Pto-050. **l**, DAK-Pto-051. **m**, DAK-Pto-047. **n**, DAK-Pto-045. **o**, DAK-Pto-049. a, c-d, h-i and k-l: upper incisors. b, e-g, j and m-o: lower incisors. Scale bar = 1 mm.

Fig. 3 Incisor cross-sections of Dakhla C_2 rodents from El Argoub. **a**, DAK-Arg-074. **b**, DAK-Arg-076. **c**, DAK-Arg-073. **d**, DAK-Arg-072. **e**, DAK-Arg-085. **f**, DAK-Arg-075. **g**, DAK-Arg-086. **h**, DAK-Arg-078. **i**, DAK-Arg-079. **j**, DAK-Arg-080. **k**, DAK-Arg-077. **l**, DAK-Arg-081. **m**, DAK-Arg-082. **n**, DAK-Arg-083. **o**, DAK-Arg-084. a-c, e, h-i and n: upper incisors. d, f-g, j-m and o: lower incisors. Scale bar = 1 mm.

Fig. 4 Scanning electron photomicrographs of Dakhla C_2 upper incisors of anomaluroids from Porto Rico and El Argoub, for which the enamel microstructure (uniserial HSBs) is shown in longitudinal section and at different magnifications. The left pictures illustrate an overview of the enamel layer for each specimen, and the associated right ones a detail of the microstructure in PI. **a-b**, DAK-Pto-003, very large-sized incisor (already figured in Marivaux et al., 2017a, fig. 7). **c-d**, DAK-Arg-073, large-sized incisor. **e-f**, DAK-Pto-043, medium-sized incisor.

Fig. 5 Scanning electron photomicrographs of Dakhla C_2 lower incisors of hystricognaths from Porto Rico, for which the enamel microstructure (multiserial HSBs) is shown in longitudinal section and at different magnifications. The left pictures illustrate an overview of the enamel layer for each specimen, and the associated right ones a detail of the microstructure in PI. **a-b**, DAK-Pto-037, large-sized incisor; **c-d**, DAK-Pto-041, medium-sized incisor. **e-f**, DAK-Pto-044, medium-sized incisor.

Fig. 6 Scanning electron photomicrographs of Dakhla C_2 upper incisors of hystricognaths from Porto Rico, for which the enamel microstructure (multiserial HSBs) is shown in longitudinal section and at different magnifications. The left pictures illustrate an overview of the enamel layer for each specimen, and the associated right ones a detail of the microstructure in PI. **a-b**, DAK-Pto-038, medium-sized incisor. **c-d**, DAK-Pto-046, small-sized incisor. **e-f**, DAK-Pto-048, small-sized incisor.

Fig. 7 Scanning electron photomicrographs of Dakhla C_2 lower incisors of hystricognaths from El Argoub, for which the enamel microstructure (multiserial HSBs) is shown in

longitudinal section and at different magnifications. The left pictures illustrate an overview of the enamel layer for each specimen, and the associated right ones a detail of the microstructure in PI. **a-b**, DAK-Arg-075, large-sized incisor. **c-d**, DAK-Arg-077, medium-sized incisor. **e-f**, DAK-Arg-082, small-sized incisor.

Fig. 8 Scanning electron photomicrographs of Dakhla C_2 upper incisors of hystricognaths from El Argoub, for which the enamel microstructure (multiserial HSBs) is shown in longitudinal section and at different magnifications. The left pictures illustrate an overview of the enamel layer for each specimen, and the associated right ones a detail of the microstructure in PI. **a-b**, DAK-Arg-074, large-sized incisor. **c-d**, DAK-Arg-078, medium-sized incisor. **e-f**, DAK-Arg-085, medium-sized incisor.

Table captions

Table 1 Incisor enamel characters of the studied specimens from Dakhla Porto Rico level C_2 (DAK-Pto C_2).

Table 2 Incisor enamel characters of the studied specimens from Dakhla El Argoub level C_2 (DAK-Arg C_2).

Supplementary Material

ESM 1 Incisor enamel microstructure for extant and extinct Ctenohystrica. The bibliographic references are those of the main text.

ESM 2 Incisor enamel microstructure for extant and extinct Anomaluroidea. The bibliographic references are those of the main text.

Figure 1

Click here to download Figure Fig.1-Loc-Map.tif

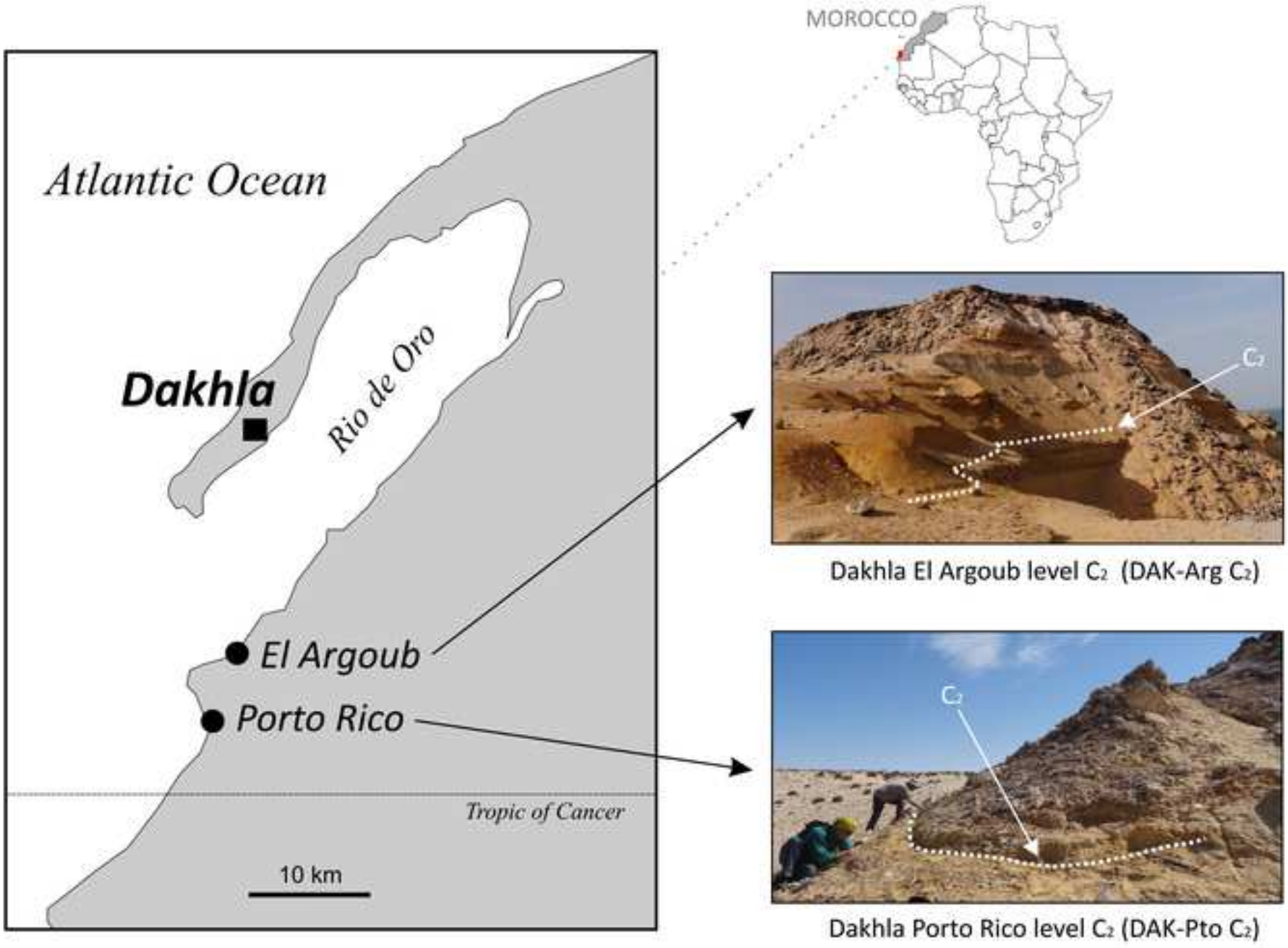

Figure 2

Click here to download Figure Fig.2-CS-Pto.tif

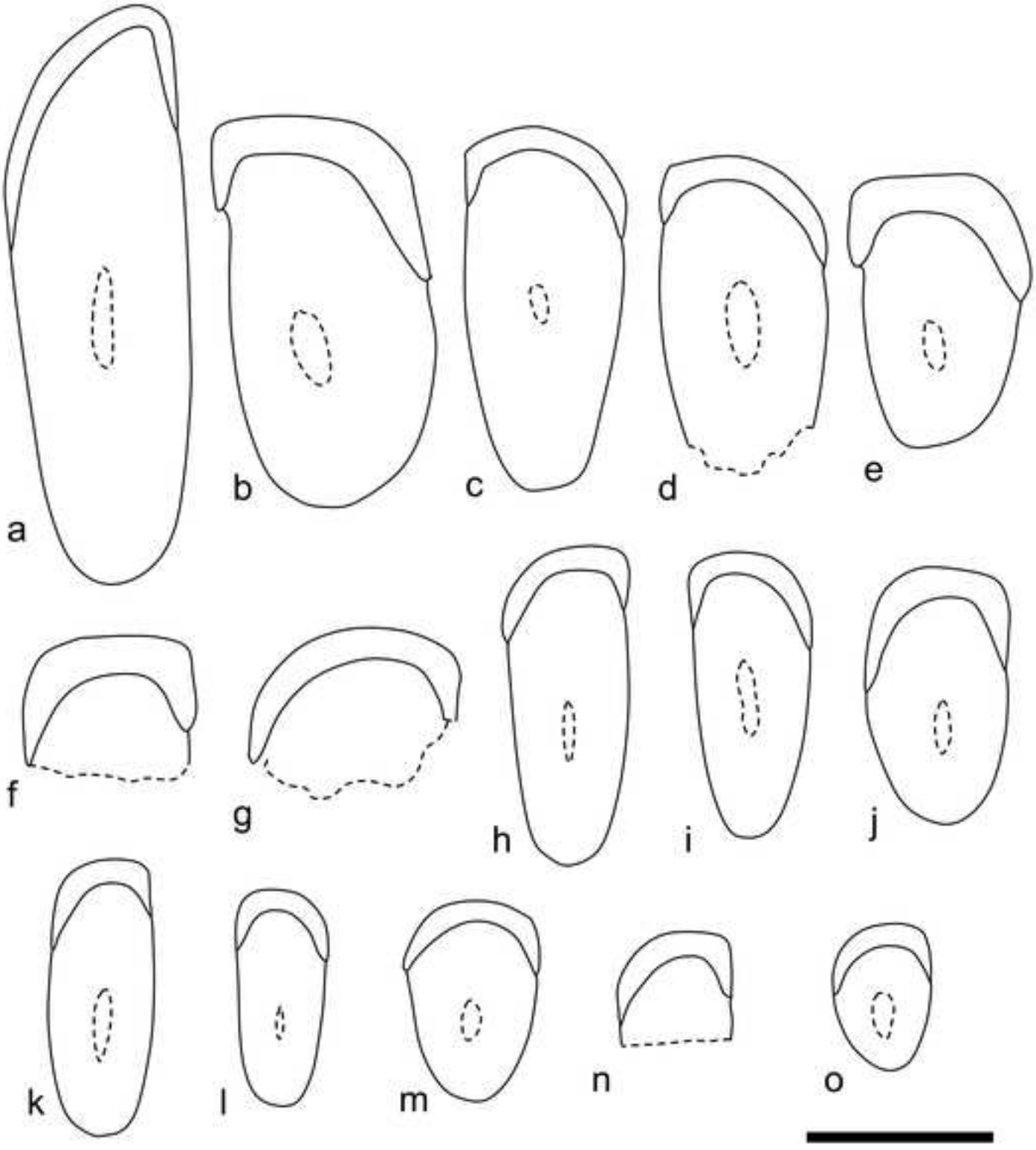

Figure 3

Click here to download Figure Fig.3-CS-Arg.tif

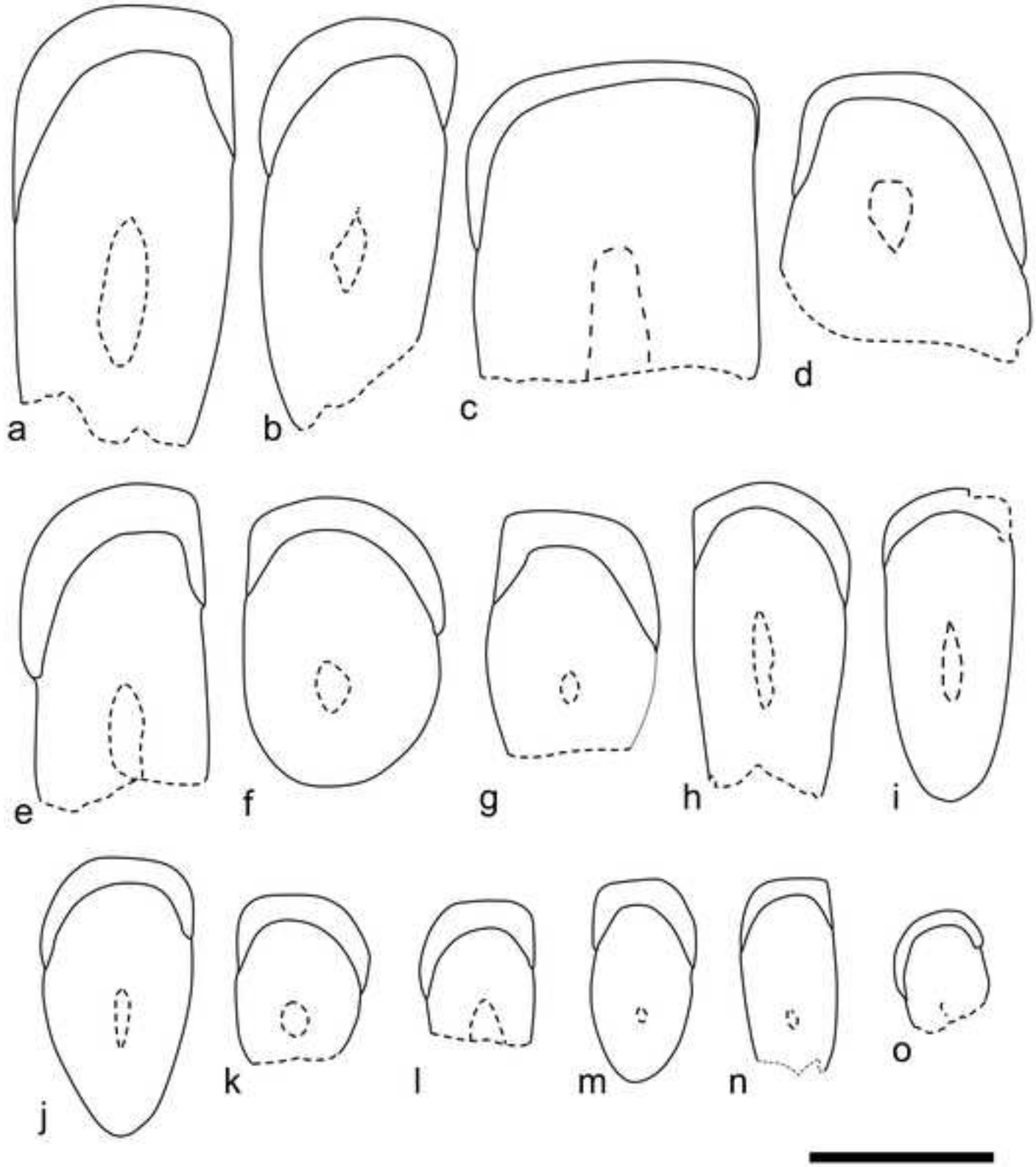

Figure 4

Click here to download Figure Fig.4-PTO-ARG-Uniserial-Upper-Inc.tif

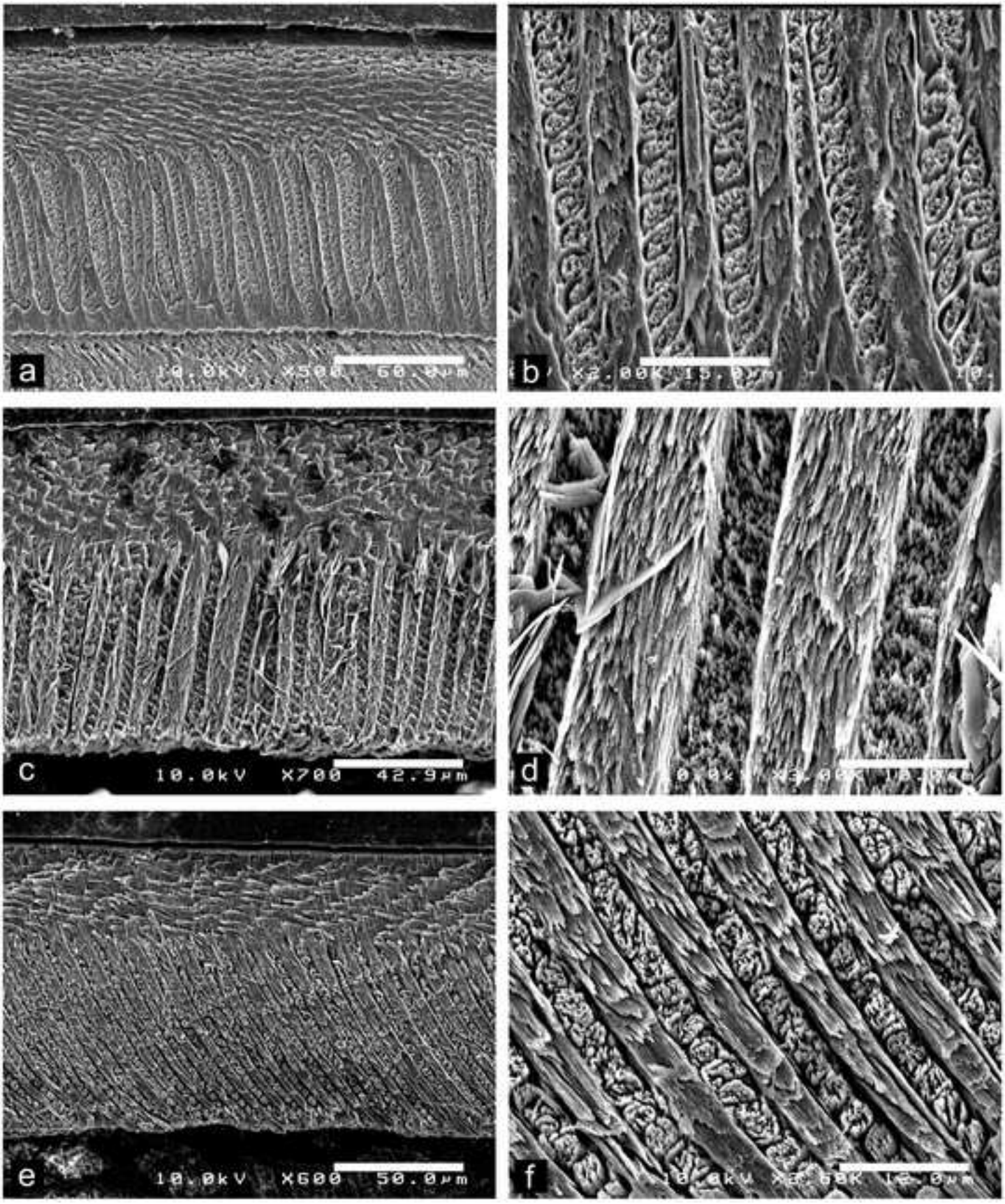

Figure 5

Click here to download Figure Fig.5-PTO-Multi-Lower-Inc.tif

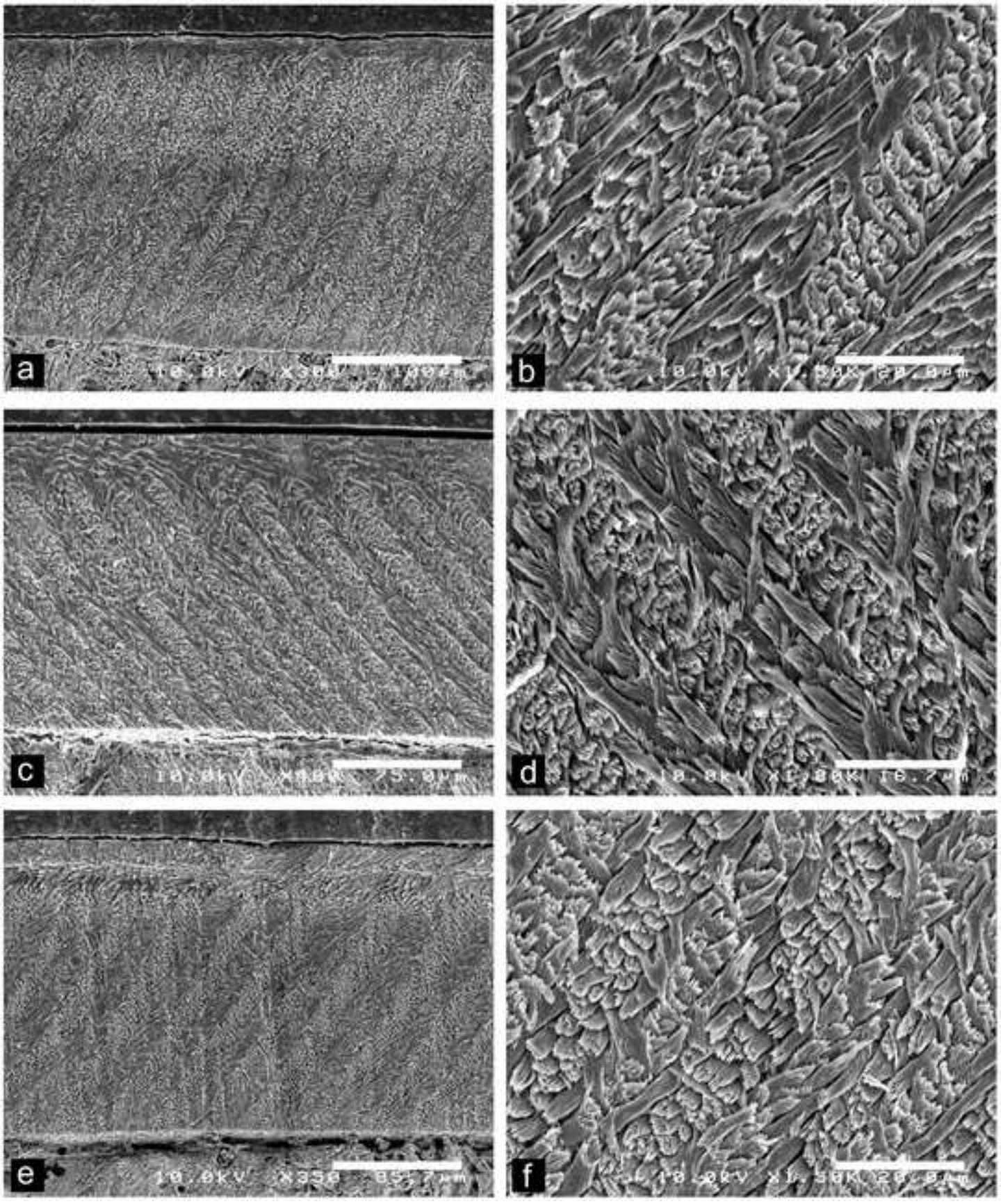

Figure 6

Click here to download Figure Fig.6-PTO-Multi-Upper-Inc.tif

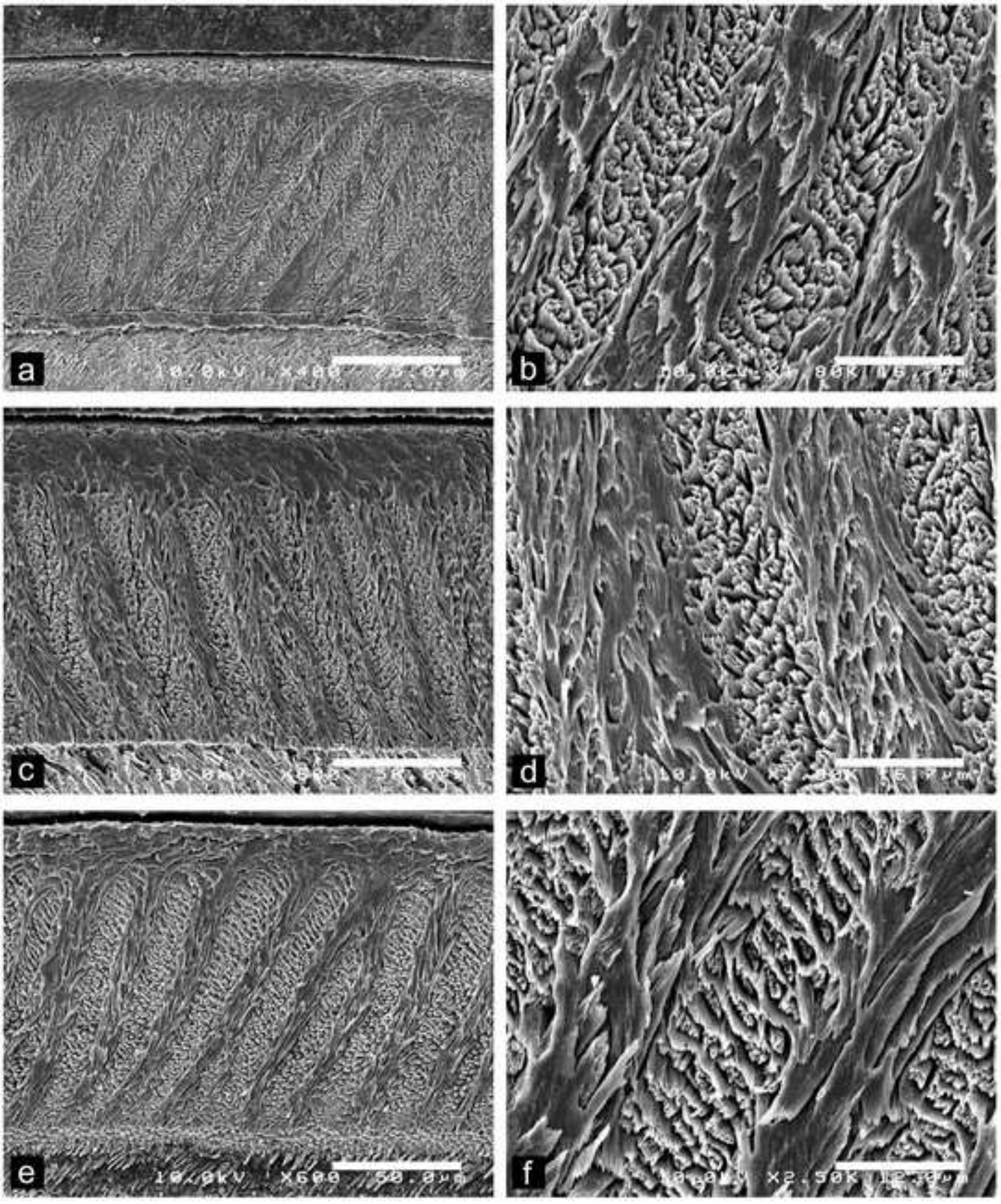

Figure 7

Click here to download Figure Fig.7-ARG-Multi-Lower-Inc.tif

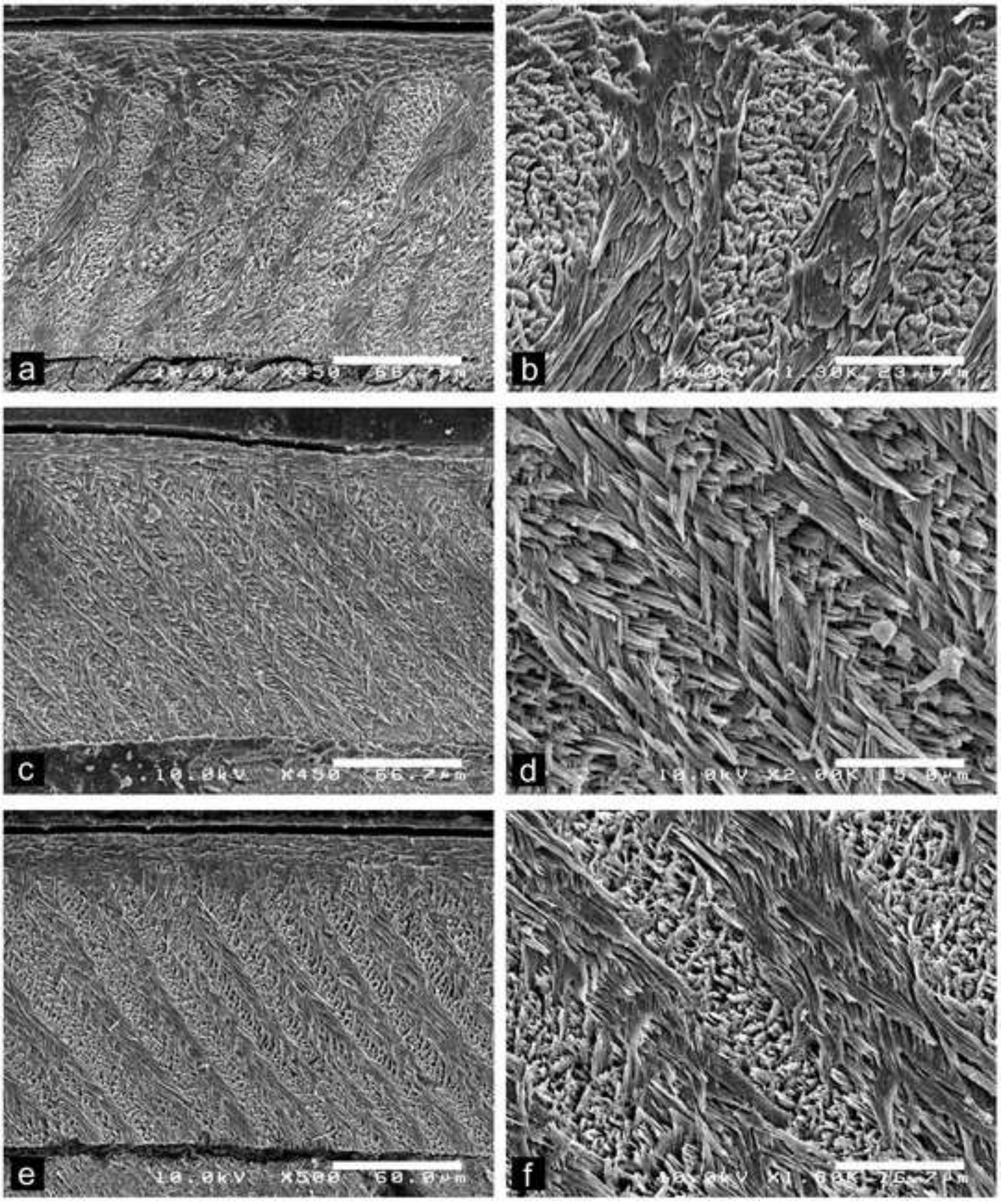

Figure 8

Click here to download Figure Fig.8-ARG-Multi-Upper-Inc.tif

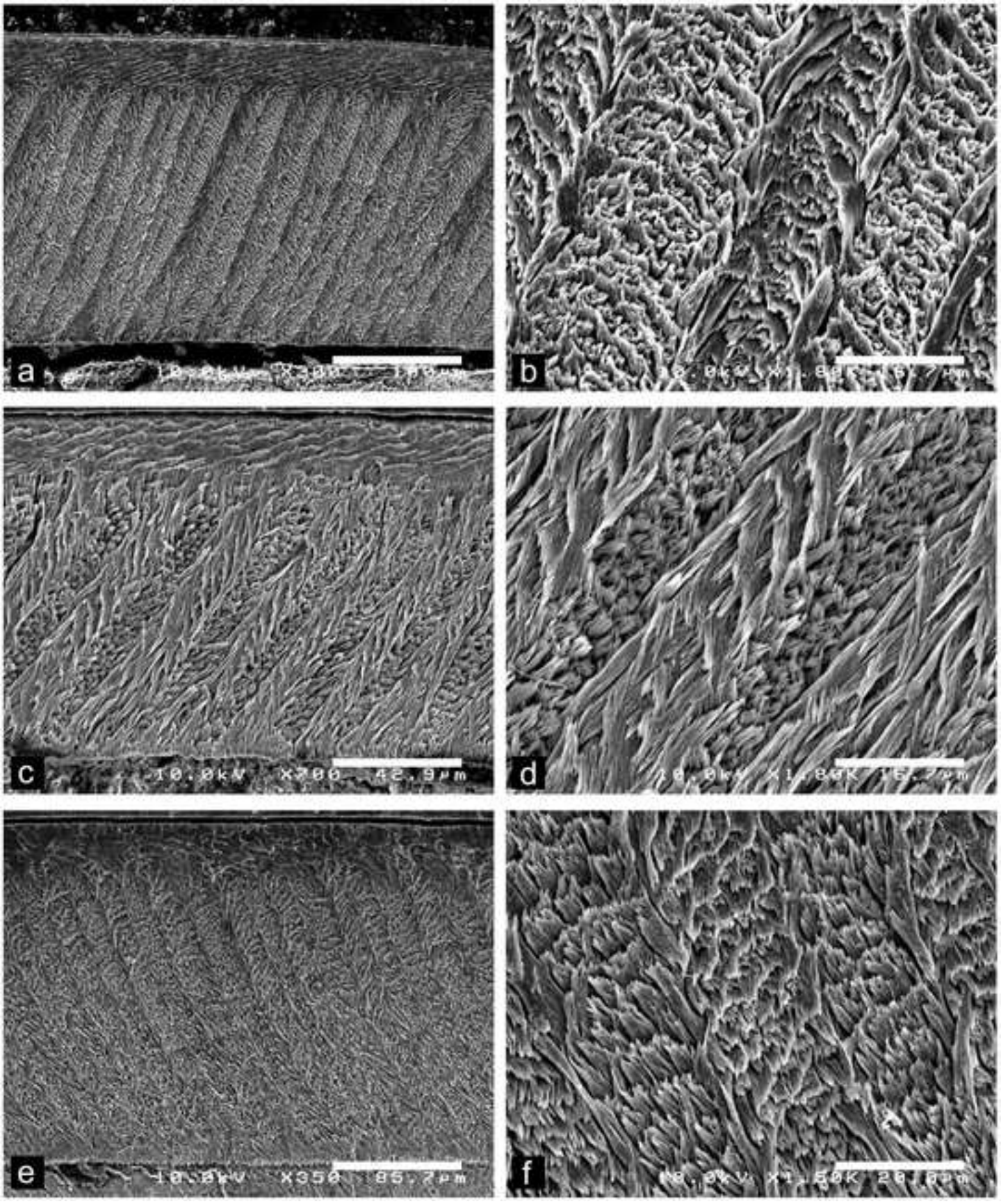

Table 1

Click here to download Table Table-1-PTO.xlsx

Specimen number	Incisor type	Incisor width (mm)	Enamel thickness (µm)	Pourcentage of PE	Inclination of prisms in PE	Inclination of HSBs	Prisms per HSB	Prisms of transitional zone	Division HSB	Prism cross section in PI	IPM configuration in PI	IPM anastomose	Angle crystallites of IPM and prism	Enamel type	Subtype	Figure
DAK-Pto-003	Upper	1.7	134	35	68-70°	5-10°	1-(2)	IPM sheet of transition	Possible, but infrequent	Oval to flattened	Sheet-like to sheath-like	Permanent	Parallel (0°)	Uniserial	1	4a-b
DAK-Pto-037	Lower	1.1	257	9	70°	30°	3-4	Well-marked	Absent	Oval	Sheet-like	Frequent and regular	Acute (50-53°)	Multiserial	2	5a-b
DAK-Pto-042	Lower	1.1	161	13	71°	33°	4	Well-marked	Absent	Flattened	Sheet-like	Frequent and regular	Acute (40-42°)	Multiserial	2	-
DAK-Pto-039	Upper	0.9	126	19	57°	18°	3-4	Absent	Possible, but infrequent	Flattened	Sheet-like	Frequent and regular	Acute (23-30°)	Multiserial	2	-
DAK-Pto-041	Lower	0.9	176	18	64°	36°	4	Well-marked	Absent	Oval	Sheet-like	Frequent and regular	Acute (43-48°)	Multiserial	2	5c-d
DAK-Pto-043	Upper	0.9	112	32	77°	55-57°	1	Absent	Absent	Round	Sheet-like to sheath-like	Not frequent and irregular	Parallel (0°)	Uniserial	1	4e-f
DAK-Pto-044	Lower	0.9	196	15	62°	34°	3-4	Present, but not well-marked	Possible, but infrequent	Oval	Sheet-like	Rare	Acute (50-55°)	Multiserial	2	5e-f
DAK-Pto-038	Upper	0.8	147	23	60°	23-31°	3-4	Absent	Absent	Round	Sheet-like	Very frequent and regular	Acute (23°)	Multiserial	(1)-2	6a-b
DAK-Pto-040	Lower	0.7	195	15	80-86°	25°	3-4	Absent	Frequent	Flattened	Sheet-like	Frequent and regular	Acute (32-42°)	Multiserial	2	-
DAK-Pto-047	Lower	0.7	145	16	90°	32-37°	3-5	Absent	Frequent	Flattened	Sheet-like	Frequent and regular	Acute (36-43°)	Multiserial	2	-
DAK-Pto-045	Lower	0.6	162	16	79°	36°	3-4	Absent	Possible, but infrequent	Round to oval	Sheet-like	Frequent and regular	Acute (34-39°)	Multiserial	2	-
DAK-Pto-046	Upper	0.6	125	23	50-55°	21°	4	Absent	Possible, but infrequent	Oval to flattened	Sheet-like to sheath-like	Very frequent and regular	Acute (23-33°)	Multiserial	2	6c-d
DAK-Pto-048	Upper	0.6	125	20	63°	25-31°	3-4	Absent	Possible, but infrequent	Flattened	Sheet-like	Very frequent and regular	Acute (28-35°)	Multiserial	2	6e-f
DAK-Pto-049	Lower	0.5	108	19	90°	33-34°	4	Well-marked	Absent	Flattened	Sheet-like	Rare	Acute (60°)	Multiserial	2	-
DAK-Pto-050	Upper	0.5	112	15	90°	23°	?4	Present, but not well-marked	Absent	Flattened	Sheet-like to sheath-like	Very frequent and regular	Acute (23°)	Multiserial	(1)-2	-
DAK-Pto-051	Upper	0.5	98	14	72°	23°	(3)-4	Absent	Absent	Flattened	Sheet-like	Frequent and regular	Acute (30-35°)	Multiserial	2	-

Table 2

Click here to download Table Table-2-ARG.xlsx

Specimen number	Incisor type	Incisor width (mm)	Enamel thickness (µm)	Pourcentage of PE	Inclination of prisms in PE	Inclination of HSBs	Prisms per HSB	Prisms of transitional zone	Division HSB	Prism cross section in PI	IPM configuration in PI	IPM anastomose	Angle crystallites of IPM and prism	Enamel type	Subtype	Figure
DAK-Arg-073	Upper	1.6	109	41	90°	6°	1-(2)	Absent	Absent	Flattened	Sheet-like to sheath-like	Permanent	Parallel (0°)	Uniserial	1	4c-d
DAK-Arg-072	Lower	1.3	117	31	38°	7-15°	3-4	Absent	Possible, but infrequent	?	?	?	?	Multiserial	?	-
DAK-Arg-074	Upper	1.1	240	17	70°	24°	4-5	Well-marked	Possible, but infrequent	Flattened	Sheet-like	Frequent and regular	Acute (19-35°)	Multiserial	2	8a-b
DAK-Arg-075	Lower	1.1	170	20	76°	23°	3-4	Absent	Possible, but infrequent	Oval	Sheet-like	Frequent and regular	Acute (33-40°)	Multiserial	2	7a-b
DAK-Arg-076	Upper	1.0	217	14	84°	25°	5-6	Present, but not well-marked	Possible, but infrequent	Oval	Sheet-like	Frequent and regular	Acute (23-36°)	Multiserial	2	-
DAK-Arg-085	Upper	0.9	229	17	70°	27°	5-6	Well-marked	Absent	Oval to flattened	Sheet-like	Frequent and regular	Acute (25-30°)	Multiserial	2	8e-f
DAK-Arg-086	Lower	0.9	185	14	66°	40°	4	Well-marked	Absent	Flattened	Sheet-like	Frequent and regular	Acute (39-50°)	Multiserial	2	-
DAK-Arg-078	Upper	0.8	115	17	71°	36-37°	3-4	Infrequent and scarce	Absent	Oval	Sheet-like	Very frequent and regular	Acute (34-38°)	Multiserial	2	8c-d
DAK-Arg-080	Lower	0.8	131	17	55°	30°	3-4	Well-marked	Absent	Oval	Sheet-like	Frequent and regular	Acute (40°)	Multiserial	2	-
DAK-Arg-077	Lower	0.7	161	10	90°	38-40°	3-4	Absent	Absent	?	Sheet-like	Rare	Acute (43-56°)	Multiserial	2	7c-d
DAK-Arg-079	Upper	0.7	110	20	66°	32-34°	3-5	Well-marked	Possible, but infrequent	Oval	Sheet-like	Frequent and regular	Acute (30-40°)	Multiserial	2	-
DAK-Arg-081	Lower	0.6	168	14	?	30-35°	3-4	Absent	Possible, but infrequent	Flattened	Sheet-like	Rare	Acute 40-45°)	Multiserial	2	-
DAK-Arg-082	Lower	0.5	148	16	84°	34-36°	(3)-4	Absent	Frequent	Flattened	Sheet-like	Frequent and regular	Acute (35-53°)	Multiserial	2	7e-f
DAK-Arg-083	Upper	0.5	90	20	63°	25°	3-4	Absent	?	Oval to flattened	Sheet-like	Frequent and regular	Acute (34°)	Multiserial	2	-
DAK-Arg-084	Lower	0.5	98 (but eroded)	NA	?	28°	3-4	Absent	Absent	?	Sheet-like	Frequent and regular	Acute (40-50°)	Multiserial	2	-